# A PDF/NPF Neuropeptide Signaling Circuitry of Male *Drosophila melanogaster* Controls Rival-Induced Prolonged Mating

Woo Jae Kim,[1] Lily Yeh Jan,[1] and Yuh Nung Jan[1,*]
[1]Howard Hughes Medical Institute, Departments of Physiology, Biochemistry, and Biophysics, University of California, San Francisco, San Francisco, CA 94158, USA
*Correspondence: yuhnung.jan@ucsf.edu
http://dx.doi.org/10.1016/j.neuron.2013.09.034

## SUMMARY

A primary function of males for many species involves mating with females for reproduction. *Drosophila melanogaster* males respond to the presence of other males by prolonging mating duration to increase the chance of passing on their genes. To understand the basis of such complex behaviors, we examine the genetic network and neural circuits that regulate rival-induced Longer-Mating-Duration (LMD). Here, we identify a small subset of clock neurons in the male brain that regulate LMD via neuropeptide signaling. LMD requires the function of pigment-dispersing factor (PDF) in four s-LNv neurons and its receptor PDFR in two LNd neurons per hemisphere, as well as the function of neuropeptide F (NPF) in two neurons within the sexually dimorphic LNd region and its receptor NPFR1 in four s-LNv neurons per hemisphere. Moreover, rival exposure modifies the neuronal activities of a subset of clock neurons involved in neuropeptide signaling for LMD.

## INTRODUCTION

A primary function of the male sex is to mate with the female to propagate their genes. Male sexual behavior includes copulation and preceding behaviors to locate and detect a female, assess her suitability, and induce her to respond receptively. Notably, *Drosophila melanogaster* males react to the presence of other males by prolonging the mating duration to increase their paternity share in the progeny (Bretman et al., 2009, 2010). Our previous study has revealed that rival-induced prolonged mating, namely, Longer-Mating-Duration (LMD), is a plastic behavior dependent on a male's social context. LMD requires visual input and depends on the activity of a subset of circadian clock neurons that are known to express neuropeptides (Kim et al., 2012), raising the question about the role of neuropeptide signaling in LMD.

Neuropeptides regulate development, growth, feeding, metabolism, reproduction, homeostasis, and longevity and modulate olfaction, locomotor control, learning, and memory (Nässel, 2000; Nässel and Winther, 2010). Studies of neuropeptides and their receptors as mediators of social behaviors provide one entry point for exploring the "dark matter"—the underlying cellular basis—of social neuroscience (Insel, 2010). Moreover, neuropeptide modulation of behavioral plasticity is likely an ancient form of neuronal signaling conserved among vertebrates and invertebrates (Beets et al., 2012; Choi et al., 2013; Garrison et al., 2012).

Clock neurons in the fly brain secrete several kinds of neuropeptides (see Figure 1A and Figure S1A [available online] for neurons relevant to our study). The first output messenger identified in insect clock neurons is the neuropeptide PDF, utilized by five large lateral ventral clock neurons (l-LNvs) and four of the five small lateral ventral neurons (s-LNvs) in the adult brain hemisphere of *Drosophila* (Renn et al., 1999). The fifth s-LNv is in close proximity to the l-LNvs and lacks PDF expression. The lateral dorsal neurons (LNds) are located more dorsally and represent a heterogeneous six-cell cluster per hemisphere expressing different neurotransmitters, such as acetylcholine (indicated by the presence of the choline acetyltransferase), ion transporter peptide (ITP), and the long or short form of neuropeptide F (NPF and sNPF).

Neuropeptide F (NPF or dNPF) shares sequence similarities with the vertebrate neuropeptide Y (NPY) family of peptides that end with tyrosine (Y) amide; NPFs end with phenylalanine (F). In *Drosophila*, the most prominent NPF-expressing neurons are two large neurons in the protocerebrum per hemisphere that project extensive processes all over the dorsal brain (Krashes et al., 2009). There are ten NPF neurons in the female fly brain hemisphere and 13 NPF neurons in the male fly brain hemisphere, including three LNds with male-specific NPF expression; there appear to be no NPF-expressing neurons in the ventral nerve cord (Hermann et al., 2012; Lee et al., 2006).

Neuropeptides bind to receptors of high affinity; hence, it is possible for neurons to release neuropeptides and signal other neurons that express the appropriate receptors even if there are no synaptic contacts (Jan and Jan, 1982; Nässel and Winther, 2010). Therefore, for the elucidation of neuropeptide signaling for a specific behavior, it is necessary to identify not only the relevant neuropeptide and receptor but also the neurons that mediate the neuropeptide signaling for the behavior regardless whether they are in synaptic contacts.

The PDF receptor PDFR belongs to the class II (class B) G-protein-coupled receptors (GPCRs) (Hyun et al., 2005; Lear et al.,
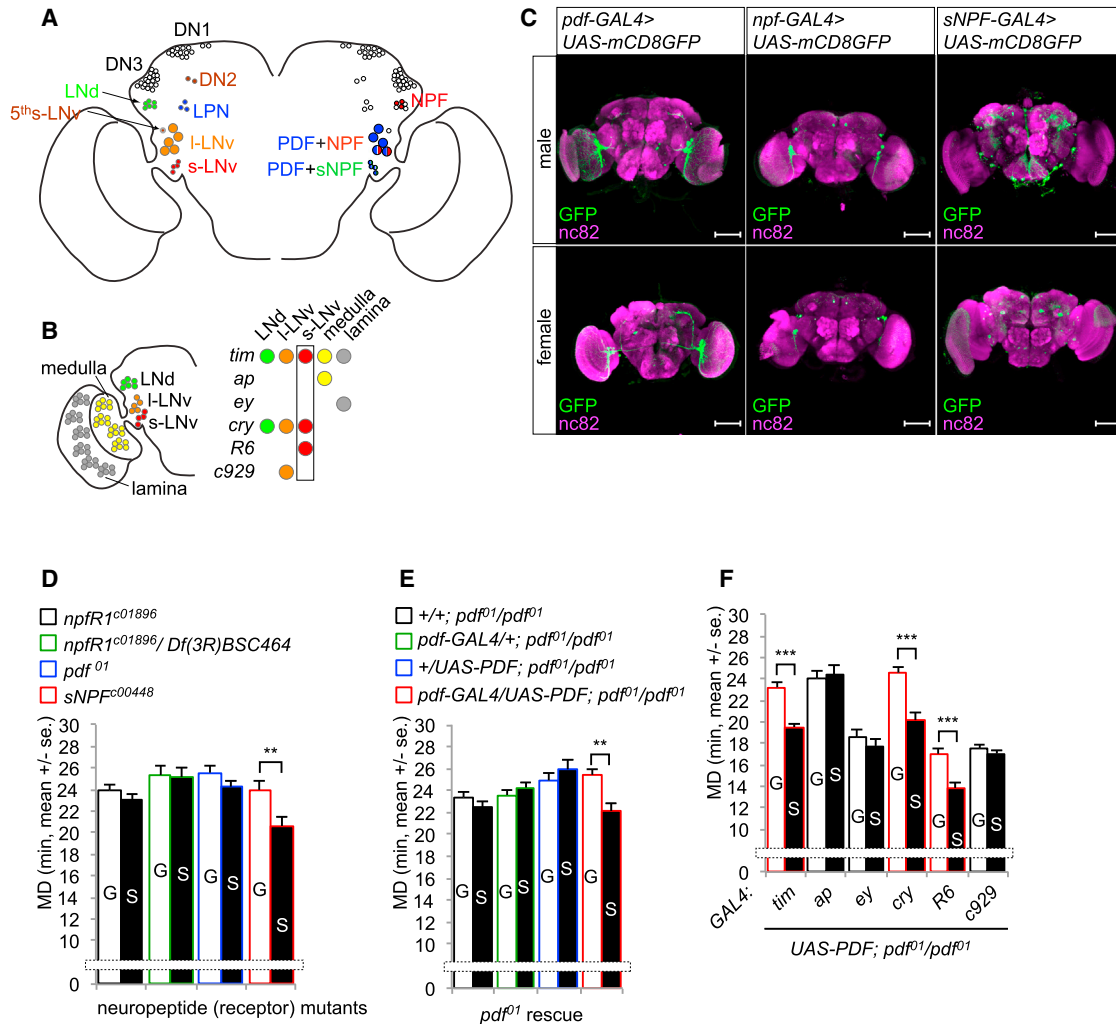
**Figure 1. PDF and NPF Are Required to Generate LMD Behavior**

(A) Clock neurons (Choi and Nitabach, 2010) and their neuropeptide expression.

(B) PDF expression in s-LNv neurons is necessary and sufficient for LMD. Subsets of neurons labeled by *GAL4* drivers named in italic are color-coded. See Figures S1A and S1B for a summary of *GAL4* drivers.

(C) Male (top) and female (bottom) flies expressing *pdf-GAL4*, *npf-GAL4* or *sNPF-GAL4* together with *UAS-mCD8GFP* were immunostained with anti-GFP (green) and nc82 (magenta) antibodies. Scale bars represent 100 μm.

(D) Mating duration assays of neuropeptide or receptor mutants. G, group-reared; S, singly reared males. See Figures S1D and S1E for controls revealing normal courtship latency and indices of these mutants.

(E and F) Mating duration assays of *pdf* rescue experiments. The genotypes are color-coded in (D) and (E) as specified above the bar graphs and are indicated below the bar graphs in (E) and (F) (red marks indicate significant rescue in F). Bars represent mean of the mating duration (MD) with error bars representing the SEM. Asterisks represent significant differences revealed by Student's t test (*p < 0.05, **p < 0.01, ***p < 0.001). The same symbols for statistical significance are used in all other figures.

2005; Mertens et al., 2005). In the *Drosophila* brain, subsets of clock neurons express PDFR (Im et al., 2011; Im and Taghert, 2010). One receptor for NPF (CG10342; *npfR1*) in *Drosophila* (Garczynski et al., 2002; Wen et al., 2005) regulates foraging, feeding, alcohol sensitivity, aggression, and sexual dimorphism in circadian locomotor activity (Chen et al., 2008; Dierick and Greenspan, 2007; Krashes et al., 2009; Lee et al., 2006; Lingo et al., 2007; Shen and Cai, 2001; Shohat-Ophir et al., 2012; Wen et al., 2005; Wu et al., 2003, 2005a, 2005b). An important aspect of neuropeptide modulation that has not been extensively

studied concerns how neuropeptides, such as PDF, contribute to socially modifiable behaviors (Taghert and Nitabach, 2012).

In this study, we show that both PDF and NPF neuropeptides regulate Longer-Mating-Duration of male flies. In addition to delineating the requisite circuitry by identifying the neurons that express neuropeptide receptors PDFR and NPFR1 to mediate rival-induced prolongation of mating duration, our study has uncovered a number of sexually dimorphic arrangements in the neuronal circuitries, as well as a strong influence of rival exposure over the activities of central neurons, including those

implicated in neuromodulation of rival-induced prolonged mating duration.

## RESULTS

### LMD Requires the Neuropeptides PDF and NPF, but Not sNPF

Longer-Mating-Duration (LMD) is a plastic response of *Drosophila* males to rivals. When males are housed together with rivals for 5 days before mating, they prolong their mating duration as compared to socially isolated males. Our previous study has found that LMD requires a subset of PDF-expressing neurons (Kim et al., 2012), including s-LNvs and l-LNvs that express not only PDF but also NPF or sNPF (Figure 1A). The relevant *GAL4* driver for each of these three neuropeptides labels a subset of cells in the fly brain (Figures 1B and S1B). Unlike *pdf-GAL4* and *npf-GAL4* drivers, *sNPF-GAL4* expression displayed sexual dimorphism (Figure 1C). To test for possible involvement of these neuropeptides, we performed mating duration assays with mutants lacking the neuropeptide or its receptor. Because no *npf* mutant alleles are available (Nitabach and Taghert, 2008), we tested *npfR1* mutants (Burke et al., 2012; Krashes et al., 2009). *sNPF* mutant males (Lee et al., 2008), but not *npfR1* mutant males or *pdf* mutant males, displayed LMD (Figure 1D). In light of the normal courtship index and latency of *pdf* and *npfR1* mutant males (Figures S1D and S1E), PDF and NPF signaling specifically affects LMD rather than the general courtship behavior. These results reveal that the LMD behavior requires the neuropeptides PDF and NPF, but not sNPF.

### LMD Requires PDF Expression in Four s-LNv Neurons

To identify the neurons that express PDF to mediate LMD, we used different *GAL4* drivers to express PDF in various subsets of the ~150 clock neurons in *pdf* mutants (Figure S1B). LMD was restored in *pdf01* mutants expressing the *UAS-PDF* transgene via *pdf-GAL4* driver (Figure 1E), as expected. Expressing PDF broadly in clock neurons via *tim-GAL4* or *cry-GAL4* also reinstated LMD in *pdf01* mutants (Figure 1F), whereas expressing the *UAS-PDF* transgene within the compound eye via *ap-GAL4* or *ey-GAL4* was insufficient to restore LMD in *pdf01* mutants (Figure 1F). Moreover, expression of *UAS-PDF* transgene in s-LNvs via *R6-GAL4*, but not in l-LNvs via *c929-GAL4*, restored LMD in *pdf01* mutants (Figure 1F). These studies reveal that PDF expression in s-LNvs is sufficient to generate LMD (Figure 1B).

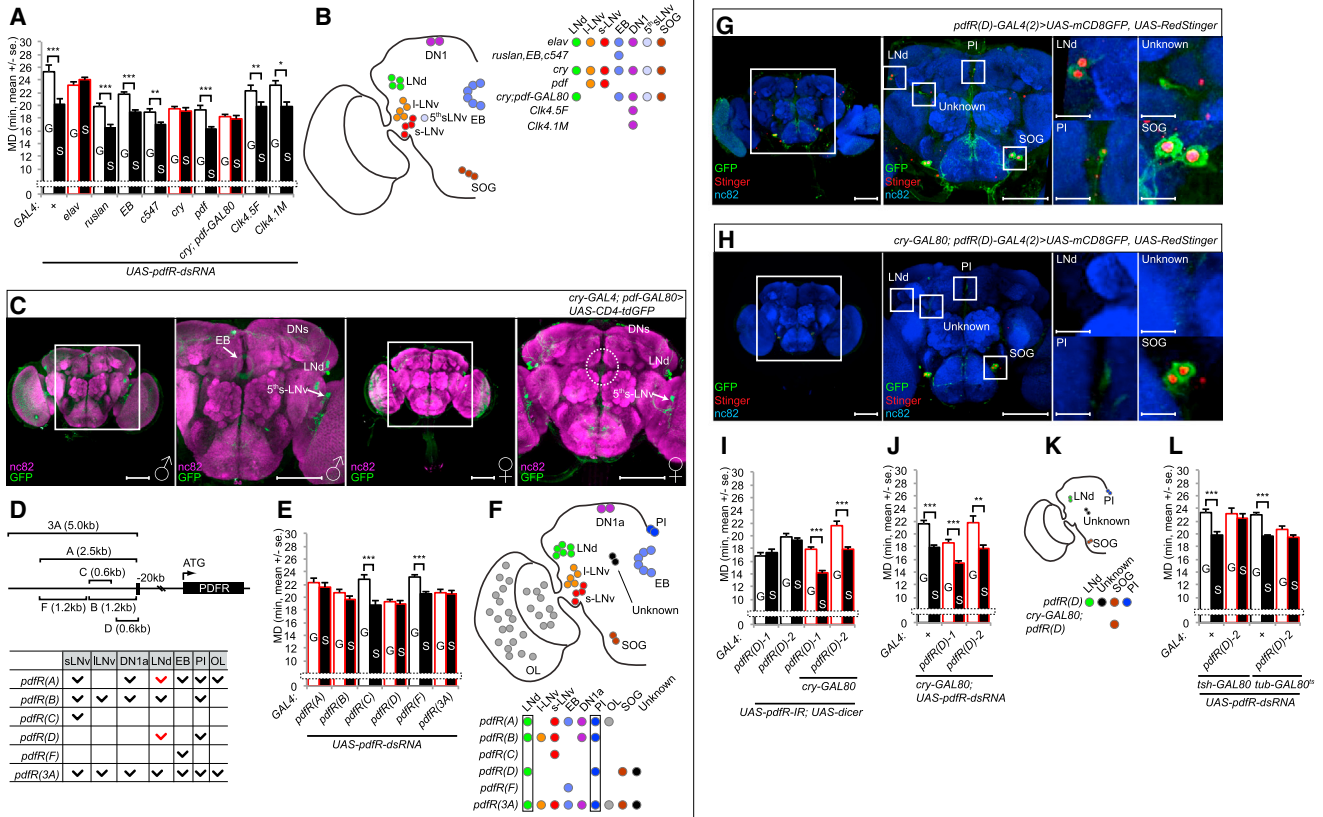### LMD Requires PDFR Expression in Two LNd Neurons that Express CRY

To identify those *pdfR*-expressing neurons required to generate LMD, we used two independent *pdfR-siRNA* lines (*UAS-pdfR-dsRNA* or *UAS-pdfR-IR*) in combination with various *GAL4* drivers to knock down *pdfR* expression in the *GAL4*-expressing cells (Figure S1B). LMD was abolished by expression of *pdfR-siRNA* in all neurons (via the panneuronal *elav-GAL4* driver), but not in the ellipsoid body (EB) neurons (Figures 2A and S2C), notwithstanding the expression of *pdfR-GAL4* drivers in the EB (Im and Taghert, 2010; Parisky et al., 2008). Whereas LMD remained intact with expression of *pdfR-siRNA* in the

PDF-expressing neurons (via *pdf-GAL4*) or in a subset of dorsal neurons (via *Clk4.1M-GAL4* or *Clk4.5F-GAL4* drivers), LMD was abolished by expression of *pdfR-siRNA* in CRY-positive cells, which include most of the lateral neurons and a small subset of dorsal neurons (Figures 2A and S2C). Furthermore, knockdown of *pdfR* expression in CRY-positive and PDF-negative cells using *cry-GAL4; pdf-GAL80* driver was sufficient to disrupt LMD (*cry; pdf-GAL80* in Figures 2A and S2C). Thus, PDFR expression in neurons that express CRY, but not PDF, is required for LMD.

To identify those neurons that must express PDFR to mediate the LMD, we characterized the expression pattern driven by the *cry-GAL4; pdf-GAL80* driver using the reporter *UAS-CD4-tdGFP* (a cell membrane marker) (Figure 2C) (Han et al., 2011), *UAS-Denmark* (a dendritic marker) together with *UAS-sytGFP* (a presynaptic marker) (Figure S2A) (Nicolaï et al., 2010), or *UAS-RedStinger* (a nuclear marker) (Figure S2B). We identified ~20–25 cells that are labeled by the *cry-GAL4; pdf-GAL80* driver, including four LNds, the fifth s-LNv, a subset of dorsal cluster neurons, and neurons in the SOG (subesophageal ganglion) and the EB in the male fly brain (Figures 2C and S2A), indicating the *pdfR* activity in these ~20–25 clock neurons per hemisphere is important for LMD (Figure 2B).

These CRY-positive, but PDF-negative, neurons appear to be in brain regions interconnected via their processes. The processes of neurons expressing reporters driven by *cry-GAL4; pdf-GAL80* bridged the LNds and the fifth s-LNv (Figures 2C and S2A). The *UAS-CD4-tdGFP* expression in the EB of male fly brains (Figure 2C) corresponds to presynaptic terminals of neurons labeled by the *cry-GAL4; pdf-GAL80* driver, because the *UAS-sytGFP* expression via this driver gave a similar pattern in the EB (Figure S2A). Sexual dimorphism is evident from the absence of such neuronal projection in the EB of the female brain (Figure 2C) and from the presence of four CRY-positive LNd neurons in the male brain but only two in the female brain (Figure S2B). The male-specific projection of CRY-positive neurons to the EB is of particular interest, in light of the requirement of the EB for visual memory to generate LMD (Kim et al., 2012).

To further narrow down the *pdfR*-expressing neurons involved in LMD, we used different *pdfR-GAL4* lines to knock down the *pdfR* expression in small subsets of neurons (Figure 2D). RNAi-mediated *pdfR* knock down via *pdfR(C)-GAL4* or *pdfR(F)-GAL4*, which drives expression in the s-LNv or EB (Figures S2M and S2N), had no effect on LMD (Figures 2E and S2Q). Of the *GAL4* drivers that were effective in suppressing *pdfR* expression to eliminate LMD, the *pdfR(D)-GAL4* driver contains a minimal region of the *pdfR*-promoter (Figure 2D). Among two independent insertion lines, *pdfR(D)-GAL4(1)* and *pdfR(D)-GAL4(2)*, we chose *pdfR(D)-GAL4(2)* because this driver labels a smaller number of cells (Figure S2O). The 15 cells per brain that are labeled by *pdfR(D)-GAL4(2)* can be divided into four different subsets of cells in both the male (Figure 2G) and female brains (Figure S2E): two LNds, three SOG neurons and two uncharacterized neurons near the antennal lobe (AL) per hemisphere, and one neuron in the central PI (pars intercerebralis) (Figure 2G). When this *GAL4* driver was combined with *cry-GAL80*, *UAS-mCD8GFP* and *UAS-RedStinger*, expression was restricted to the SOG region (Figure 2H). Expression of *pdfR-siRNA* by *pdfR(D)-GAL4(1)* or *pdfR(D)-GAL4(2)* combined with

**Figure 2. *pdfR* Expression in a Subset of Clock Neurons Is Required to Generate LMD**

(A) Mating duration assays for *GAL4*-driven knockdown of PDFR via *UAS-pdfR-dsRNA*. The *GAL4* drivers are specified below the bars, and those that affect LMD are marked with red outline for (A) and (E). See Figure S2C for similar results with *UAS-pdfR-IR; UAS-dicer*.

(B) Schematic diagram of *GAL4* drivers employed in (A) to identify cells with PDFR expression important for LMD. Subsets of neurons labeled by *GAL4* drivers (in italic) are color coded.

(C) Flies bearing *cry-GAL4; pdf-GAL80* and *UAS-CD4-tdGFP* flies were immunostained with anti-GFP (green) and nc82 (magenta) antibodies to reveal neuronal projections. Enlarged images of the boxed regions are shown in the panels to the right. Scale bars represent 100 μm. See Figures S2A, S2B, and S2D for further characterization of expression patterns.

(D) A schematic of the captured promoter region in each *pdfR-GAL4* construct (Im and Taghert, 2010; Parisky et al., 2008) (top) and a summary of expression patterns (bottom: known expression marked in black and expression determined in this study marked in red).

(E) Mating duration assays for *pdfR-GAL4*-mediated knockdown of PDFR via *UAS-pdfR-dsRNA*. See Figure S2Q for similar results with *UAS-pdfR-IR; UAS-dicer*. *GAL4* control experiments are shown in Figure S2P.

(F) Implication of PDFR expression in LNd and PI neurons for LMD. Subsets of neurons labeled by *GAL4* drivers (in italic) used in (E) are color coded.

(G and H) Flies expressing *pdfR(D)-GAL4(2)* or *cry-GAL80; pdfR(D)-GAL4(2)* together with *UAS-mCD8GFP, UAS-RedStinger* were immunostained with anti-GFP (green), anti-DsRed (red), and nc82 (blue) antibodies. Scale bars represent 100 μm in the left two panels and 10 μm in the magnified right panels. See Figures S2F and S2G for additional characterization of expression patterns.

(I) Mating duration assays for *pdfR(D)-GAL4*-mediated knockdown of PDFR via *UAS-pdfR-IR; UAS-dicer*. *GAL4* and names of the *GAL4* drivers and *GAL80* are indicated below the bars, and *GAL80* combinations that did not affect LMD are marked with red outline for (I) and (J). *GAL4* control experiments are shown in Figure S3I.

(J) Mating duration assays for *pdfR(D)-GAL4* mediated knockdown of PDFR via *UAS-pdfR-dsRNA*.

(K) Schematic of cells tested in (I) and (J).

(L) Mating duration assays for *pdfR(D)-GAL4(2)*-mediated knockdown of PDFR via *UAS-pdfR-dsRNA* together with *tsh-GAL80* or *tub-GAL80^{ts}*. Names of the *GAL4* drivers and *GAL80* are indicated below the bars, and those combinations that affect LMD are marked with red outline. Mean ± SEM is shown.

*cry-GAL80* did not affect LMD (Figures 2I and 2J), indicating the PDFR expression in the SOG is not required for LMD. Using *tsh-GAL80* to block GAL4 expression in the ventral nerve cord (VNC), we confirmed that expressing *pdfr-siRNA* with the *pdfR(D)-GAL4(2)* driver within the brain is sufficient to impair LMD (Figure 2L). Adult-specific expression of *pdfR-siRNA* with

*pdfR(D)-GAL4(2)* via *tub-GAL80^{ts}* was also sufficient to impair LMD (Figure 2L). These data suggest that PDFR activity in LNd or PI cells labeled by *pdfR(D)-GAL4(2)* might modulate LMD (Figure 2F).

To validate that PDFR activity in a subset of PDFR-expressing cells is required for LMD, we used various *GAL4* drivers to
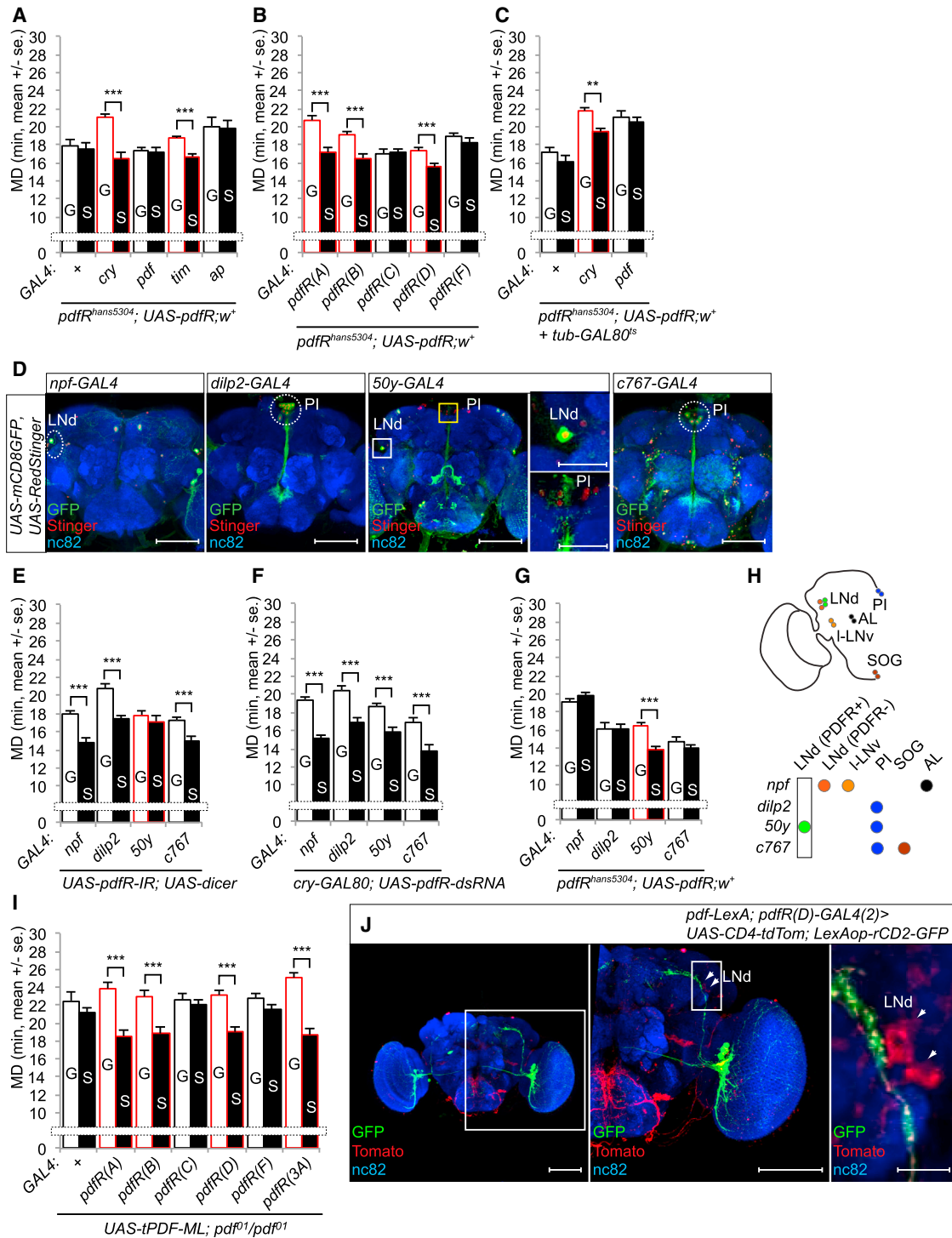
**Figure 3. *pdfR* Expression in LNd Is Required to Generate LMD**

(A and B) Mating duration assays of *pdfR* rescue experiments. Names of the *GAL4* drivers are indicated below the bars, and those that rescue LMD in *pdfR^hans5304* mutant are marked with red outline for (A)–(C).

(C) Mating duration assays of *pdfR* rescue experiments in adult-specific expression of *UAS-pdfR* transgene.

(D) Flies expressing each *GAL4* drivers together with *UAS-mCD8GFP, UAS-RedStinger* were immunostained with anti-GFP (green), anti-DsRed (red), and nc82 (blue) antibodies. White dashed circles indicate LNd and PI neurons. Scale bars represent 100 μm. See Figures S2K and S2L for additional characterization of expression patterns.

express PDFR in different subsets of clock neurons in *pdfR* mutants to see which ones can rescue the LMD phenotype. With the *pdfR* gene on the X chromosome and the $w^-$ mutation in *pdfR^hans5304* mutants, we introduced the *white* gene from a short X chromosome duplication inserted in the third chromosome to rescue the visual deficiency (Venken et al., 2010) and the LMD defects of $w^-$ mutants (Figure S3B). LMD was restored in *pdfR^hans5304* mutants expressing the *UAS-pdfR* transgene in broad clock neuron populations via *tim-GAL4* or *cry-GAL4* drivers (Figure 3A) or in a subset of PDFR-expressing neurons via the *pdfR(D)-GAL4(2)* driver (Figure 3B). However, there was no rescue of LMD if the *UAS-pdfR* transgene was expressed in PDF-expressing neurons or the visual system, by using a *pdf-GAL4* or *ap-GAL4* driver, respectively (Figures 3A and S1B). Adult-specific expression of *UAS-pdfR* transgene in CRY-positive cells using *tub-GAL80^ts* together with *cry-GAL4* was sufficient to rescue LMD in *pdfR^hans5304* mutants (Figure 3C). Thus, PDFR function in cells that express both PDFR and CRY in the adult male brain, including LNd and PI neurons, is sufficient to generate LMD (Figure 2K).

To determine which subset of cells labeled by *pdfR(D)-GAL4(2)* are required to generate LMD, we used several *GAL4* drivers that label LNd neurons or PI cells (Figure S1B). Expression of *UAS-mCD8GFP* or *UAS-RedStinger* via these *GAL4* drivers confirmed that *npf-GAL4* labels a subset of LNd neurons, but not PI cells. *dilp2-GAL4* specifically labels PI neurons, but not LNd neurons. *50y-GAL4* labels a subset of LNd neurons and PI cells. *c767-GAL4* labels a subset of PI cells, but not LNd neurons (Figures 3D and S1B). Because LMD was not affected by expressing *pdfR-siRNA* via *GAL4* drivers that label only PI cells (*dilp2-GAL4, c767-GAL4*), and *UAS-pdfR* expression via these *GAL4* drivers did not rescue the impaired LMD of *pdfR^hans5304* mutants (Figures 3E and 3G), PDFR activity in PI cells is dispensable for LMD. Only *50y-GAL4* combined with *pdfR-siRNA* was effective in abolishing LMD (Figure 3E), and expression of *UAS-pdfR* transgene with *50y-GAL4* was sufficient to rescue the impaired LMD in *pdfR^hans5304* mutants (Figure 3G). Adding *cry-GAL80* to *50y-GAL4* and *pdfR-siRNA* had no effect on LMD (Figure 3F), indicating that *pdfR* expression in CRY-positive neurons is crucial for LMD. We further confirmed that two of the LNd neurons labeled by the *50y-GAL4* driver are also CRY-positive by using *cry-GAL80* (Figures S2K and S2L). Thus, PDFR function in two CRY-positive LNd neurons labeled by the *50y-GAL4* driver, but not PI neurons labeled by *dilp2-GAL4*, *50y-GAL4*, and *c767-GAL4* drivers, is necessary and sufficient to generate LMD (Figure 3H).

## PDF Likely Diffuses to Reach PDFR-Expressing Neurons Not in Synaptic Contact with PDF-Expressing Neurons Required for LMD

PDF could be released in a paracrine fashion to activate PDFR (Hyun et al., 2005; Lear et al., 2005; Mertens et al., 2005). Because PDFR activity in two LNd neurons is necessary and sufficient to generate LMD via PDF signals from four s-LNv neurons per hemisphere, we designed additional rescue experiments with a membrane-tethered form of *PDF (UAS-tPDF-ML)* (Choi et al., 2009). Interestingly, expression of *UAS-tPDF-ML* in *pdfR(D)-GAL4(2)*-expressing cells in *pdf^01* mutants rescued the impaired LMD (Figure 3I), indicating that PDFR activation by membrane-tethered PDF expressed in a subset of PDFR-expressing cells is sufficient to generate LMD. Whereas these cells normally do not express PDF (Figure S1B), a subset of LNd neurons labeled with red fluorescence by *pdfR(D)-GAL4(2)* are in the vicinity of the PDF-expressing s-LNv neurons labeled with green fluorescence (Figure 3J). To look for evidence of synaptic contacts between LNd neurons and PDF-expressing neurons, we adopted the GFP reconstitution across synaptic partners (GRASP) approach involving the expression of two halves of a split-GFP on the cell membrane of distinct neuronal populations (Feinberg et al., 2008). Expression of one half of the split-GFP (*UAS-CD4::spGFP1-10*) under the control of *pdfR(D)-GAL4(2)* and the other half (*LexAop-CD4::spGFP11*) under the control of *pdf-LexA* did not yield GFP-positive signals (Figure S3F), in spite of the physical proximity of the dorsal horn of PDF-expressing s-LNv neurons and the cell bodies of *pdfR(D)-GAL4(2)*-labeled LNd (Figures 3J and S2G). In accordance with the hypothesis that PDF is released in a paracrine manner from varicosities (Helfrich-Förster et al., 2007), our findings suggest that PDFR in a small subset of LNd neurons may be activated by PDF released by nearby s-LNv axons that do not make direct synaptic contacts with them to generate LMD.

## LMD Requires NPFR1 Expression in the Four PDF-Positive s-LNv Neurons

Next, we asked which subsets of neurons with *npfR1* expression are required to generate LMD, by expressing *npfR1-siRNA* (*UAS-npfR1-dsRNA*) via various *GAL4* drivers (Figure S1B). Expression of *npfR1-siRNA* in all neurons (via the panneuronal *elav-GAL4* driver), but not in the EB (via the *c547-GAL4* driver) or in a subset of dorsal neurons (via the *Clk4.1M-GAL4* driver), eliminated LMD (Figure 4A). LMD was abolished by expression of *npfR1-siRNA* in the CRY-positive cells, which include most of the lateral neurons and a small subset of dorsal neurons (*cry* in Figure 4A), and by

(E) Mating duration assays for LNd- and PI-expressing *GAL4* drivers mediated knockdown of PDFR via *UAS-pdfR-IR; UAS-dicer*. Names of the *GAL4* drivers are indicated below the bars, and those that affect LMD are marked with red outline. *GAL4* control experiments are shown in Figure S3J.
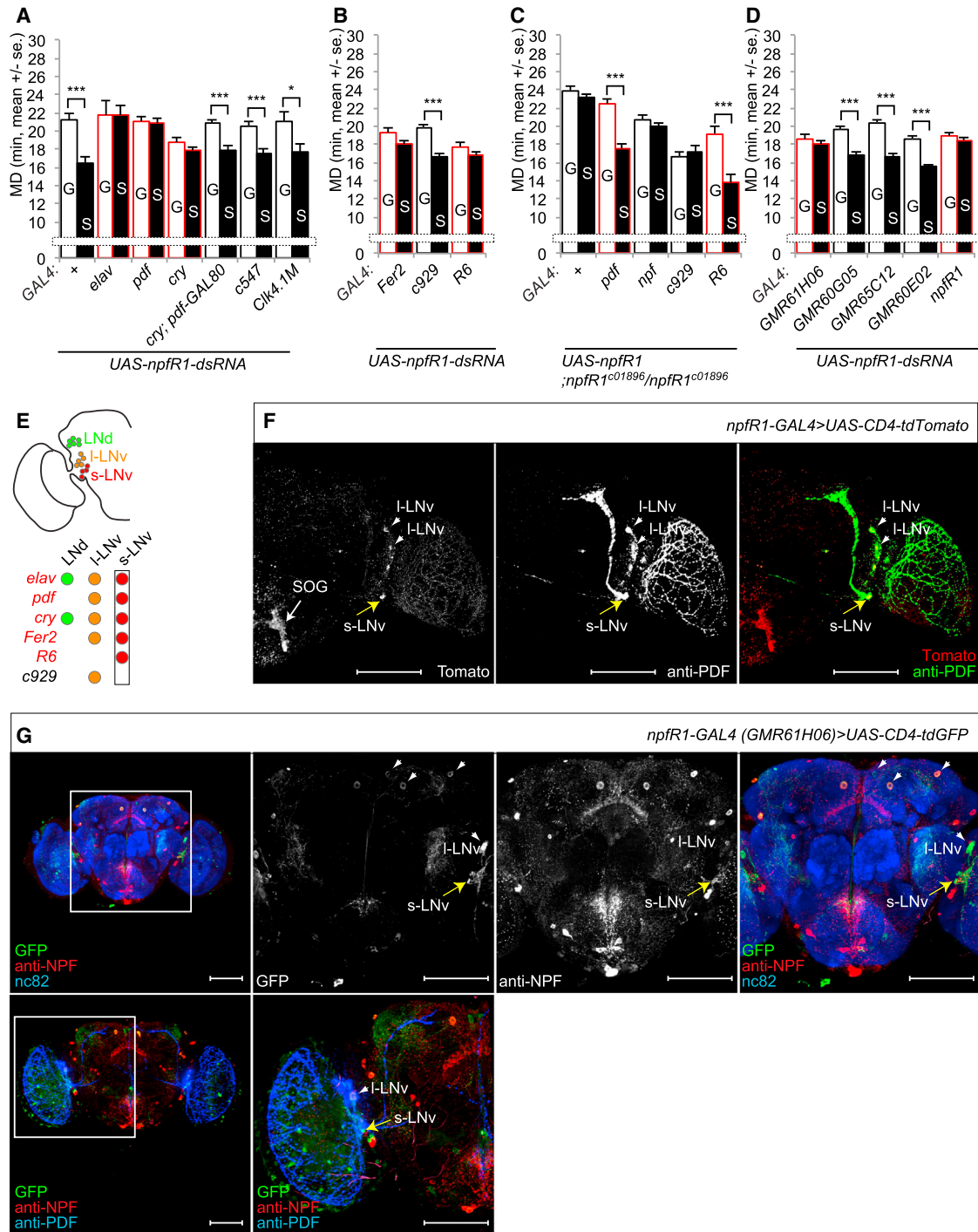
(F) Mating duration assays for LNd- and PI-expressing *GAL4* drivers mediated knockdown of PDFR in CRY-negative neurons via *cry-GAL80; UAS-pdfR-dsRNA*.

(G) Mating duration assays of *pdfR* rescue experiments with LNd- and PI-expressing *GAL4* drivers. Names of the *GAL4* drivers are indicated below the bars, and the *GAL4* driver that rescues LMD in *pdfR^hans5304* mutant is marked with red outline.

(H) Identification of LNd neurons with PDFR expression that is necessary and sufficient for LMD. Subsets of neurons labeled by *GAL4* drivers (in italic) are color coded.

(I) Mating duration assays of *pdf* rescue experiments with membrane-tethered *UAS-tPDF* transgene. *GAL4* drivers that rescue LMD in *pdf^01* mutant are marked with red outline.

(J) Flies expressing *pdf-LexA; pdfR(D)-GAL4(2)* drivers together with *UAS-CD4-tdTomato; LexAop-rCD2-GFP* were immunostained with anti-GFP (green), anti-DsRed (red), and nc82 (blue) antibodies. White arrowheads indicate LNd neurons labeled by *pdfR(D)-GAL4(2)* driver. Scale bars represent 100 μm in the left and middle panels and 10 μm in the magnified right panel. See Figure S3F for the absence of synapses detectable via GRASP. Mean ± SEM are shown.

**Figure 4.** *npfR1* **Expression in s-LNv Is Required to Generate LMD**

(A) Mating duration assays for *GAL4*-mediated knockdown of NPFR1 via *UAS-npfR1-dsRNA*. *GAL4* drivers that affect LMD are marked in red. Names of the *GAL4* drivers are indicated below the bars, and those that affect LMD are marked with red outline for (A), (B), and (D).

(B) Mating duration assays for *GAL4* drivers for NPFR1 knockdown in LNv via *UAS-npfR1-dsRNA*. *GAL4* control experiments are shown in Figure S4F.

(C) Mating duration assays of *npfR1* rescue experiments. Names of the *GAL4* drivers are indicated below the bars, and those that rescue LMD in *npfR1^{c01896}* mutant are marked with red outline.

(D) Mating duration assays for *npfR1-GAL4s*-mediated knockdown of NPFR1 via *UAS-npfR1-dsRNA*. *GAL4* control experiments are shown in Figure S4F.

(E) NPFR1 expression in s-LNv neurons is necessary and sufficient for LMD. Subsets of neurons labeled by *GAL4* drivers (in italic) are color coded.

*(legend continued on next page)*

expression of *npfR1-siRNA* in the PDF-expressing neurons (*pdf* in Figure 4A). However, knockdown of *npfR1* expression in the CRY-positive and PDF-negative cells had no effect on LMD (*cry-GAL4; pdf-GAL80* in Figure 4A). Thus, NPFR1 activity in PDF-expressing neurons is important for LMD.

To identify the PDF-expressing neurons that are important to generate LMD, we used three different *GAL4* drivers that specifically label both s-LNv and l-LNv (*Fer2-GAL4, Fer2* expression is enriched in lateral ventral neurons) (Nagoshi et al., 2010), only l-LNv (*c929-GAL4*) (O'Brien and Taghert, 1998), or only s-LNv (*R6-GAL4*) (Helfrich-Förster et al., 2007) (Figure S1B). We found that *npfR1-siRNA* expression in s-LNv (*Fer2* and *R6* in Figure 4B), but not in l-LNv (*c929* in Figure 4B), compromised LMD, indicating that the NPFR1 activity in s-LNv is necessary for LMD (Figure 4E).

To determine whether the NPFR1 activity in s-LNv is sufficient to generate LMD, we used different *GAL4* drivers to express NPFR1 in various subsets of circadian clock neurons in *npfR1* mutants. LMD was restored in *npfR1*^c01896^ mutants expressing the *UAS-npfR1* transgene in s-LNv neurons via *pdf-GAL4* or *R6-GAL4* (Figure 4C). In contrast, expression of the *UAS-npfR1* transgene in NPF-expressing neurons or only in l-LNv via *npf-GAL4* or *c929-GAL4* could not rescue the LMD (Figure 4C). Thus, the NPFR1 function in s-LNv neurons is sufficient to generate LMD (Figure 4E).

To validate the expression of various *GAL4* drivers in s-LNv neurons, we expressed *UAS-CD4-tdGFP* via the *npfR1-GAL4* driver (Wen et al., 2005). Although this *GAL4* driver produces weak expression of the fluorescence protein reporter, we confirmed the expression in s-LNv and l-LNv by using an anti-PDF antibody (Wen et al., 2005) (Figure 4F). We also collected the Janelia Farm *GAL4* lines with *GAL4* driven by the *npfR1* promoter and coding regions (Pfeiffer et al., 2008). Among these *GAL4* lines, *GMR61H06* labeled s-LNv in both male brains (Figure 4G) and female brains (Figure S4A). The other *GAL4* drivers did not label s-LNv (Figures S4B, S4C, and S4D). LMD was eliminated by expressing *npfR1-siRNA* via *npfR1-GAL4* or *GMR61H06*, but not the other *GAL4* drivers without s-LNv expression (Figure 4D). In summary, expression of NPFR1 in four PDF-positive s-LNv neurons is necessary and sufficient to generate LMD (Figure 4E).

## Two Male-Specific NPF-Expressing LNd Neurons Are Required for LMD

Sexual dimorphism of brain structure and function generates neural circuitries important for gender-specific behaviors. In *Drosophila*, *fruitless (fru)* is an essential neural sex determinant responsible for male-specific behaviors (Ryner et al., 1996). It is also well known that a subset of clock neurons is sexually dimorphic (Kadener et al., 2006; Lee et al., 2006). We therefore tested whether LMD depends on the function of a subset of sexually dimorphic LNd neurons.

To determine whether sexually dimorphic neurons are involved in LMD, we used intersectional methods to genetically dissect ∼1,500 *fru* neurons into smaller subsets. We used a combination of the *fru*^FLP^ allele that drives FLP-mediated recombination specifically in *fru* neurons with *UAS[stop]X* (X could be various reporters or effector transgenes) to express a *UAS* transgene in only those cells that are labeled by the *GAL4* driver and also *fru*-positive, due to FLP-mediated excision of the stop cassette (*[stop]*). Using *cry-GAL4; pdf-GAL80* to identify sexually dimorphic cells, we found two male-specific cells in the LNd region per hemisphere (Figure 5A). We also found that *npf-GAL4* labeled two *fru*-positive LNd neurons and two *fru*-positive cells in the antenna lobe of the male, but not female, brain (Figure 5B). In contrast, we could not find any *fru*-positive central neurons that are labeled by *dilp2-GAL4* or *pdfR(D)-GAL4(2)* drivers (Figures 5C and 5D). A subset of cells labeled by *50y-GAL4* and *c767-GAL4* drivers were *fru*-positive; however, these cells seemed unlikely to be involved given their location far from those PDF-, PDFR-, NPF-, and NFR1-expressing neurons implicated in LMD (Figures 5E and 5F). Because LNd neurons labeled by *50y-GAL4* (Figure 3D) did not emerge in the *fru*^FLP^ experiment, we concluded that the *50y-GAL4*-labeled LNd neurons are different from the NPF- and FRU-positive LNd neurons (Figure 5G).

To test whether the small subset of *fru*-positive LNd cells are involved in LMD, we expressed tetanus toxin light chain (*UAS[stop]TNT_active_*) with various *GAL4* drivers along with *fru*^FLP^ to inhibit synaptic transmission in sexually dimorphic subsets of *fru*-positive cells. As a control, we found that LMD was unaffected when we used each of these *GAL4* drivers in combination with *UAS[stop]TNT_inactive_* to express an inactive form of tetanus toxin light chain (Figure 5I). LMD was abolished by inhibition of transmitter release from *cry-GAL4; pdf-GAL80* or *npf-GAL4* labeled *fru*-positive cells, whereas blocking synaptic transmission of the other *GAL4*-labeled *fru*-positive cells did not affect LMD (Figure 5H). Similar results (Figure S3C) were obtained using the cell-autonomous toxin *Ricin A* (*UAS[stop] RicinA*), which encodes only the catalytic subunit of the toxin that can enter the cell to mediate cell ablation (Hidalgo et al., 1995). These findings indicate that LMD requires a subset of sexually dimorphic neurons labeled by *cry-GAL4; pdf-GAL80* or *npf-GAL4* drivers (Figure 5G).

Systemic expression of a female form of *tra* cDNA (*UAS-tra*^F^) in a male during development elicits female characteristics (Belote and Baker, 1987). Moreover, male-specific NPF expression is eliminated when *npf-GAL4*-labeled cells are feminized by *UAS-tra*^F^ (Lee et al., 2006). In an attempt to express *UAS-tra*^F^ under the control of various *GAL4* drivers to feminize different subsets of neurons (Figures S5A–S5G), we found that LMD was eliminated by such feminization of *cry-GAL4; pdf-GAL80*- or *npf-GAL4*-labeled cells (Figure 5J), but not by expression of

---

(F) Flies expressing *npfR1-GAL4* driver (Wen et al., 2005) together with *UAS-CD4-tdTomato* were immunostained with anti-PDF (green) and anti-DsRed (red) antibodies. White arrowheads indicate l-LNv region labeled by both *npfR1-GAL4* driver and anti-PDF antibodies. Yellow arrow indicates s-LNv region labeled by both *npfRF1-GAL4* and anti-PDF antibodies. White arrow indicates SOG region labeled by *npfRF1-GAL4*.
(G) Flies expressing *GMR61H06-GAL4* driver together with *UAS-CD4-tdTomato* were immunostained with anti-GFP (green), anti-NPF (red), and anti-nc82 (blue) antibodies (top panels) or with anti-GFP (green), anti-NPF (red), and anti-PDF (blue) antibodies (bottom panels). White arrowheads indicate l-LNv region labeled by both *GMR61H06-GAL4* driver and anti-PDF antibodies. Yellow arrow indicates s-LNv region labeled by both *GMR61H06-GAL4* and PDF antibodies. Scale bars represent 100 μm. See Figures S4A–S4D for additional characterizations of expression patterns. Mean ± SEM is shown.
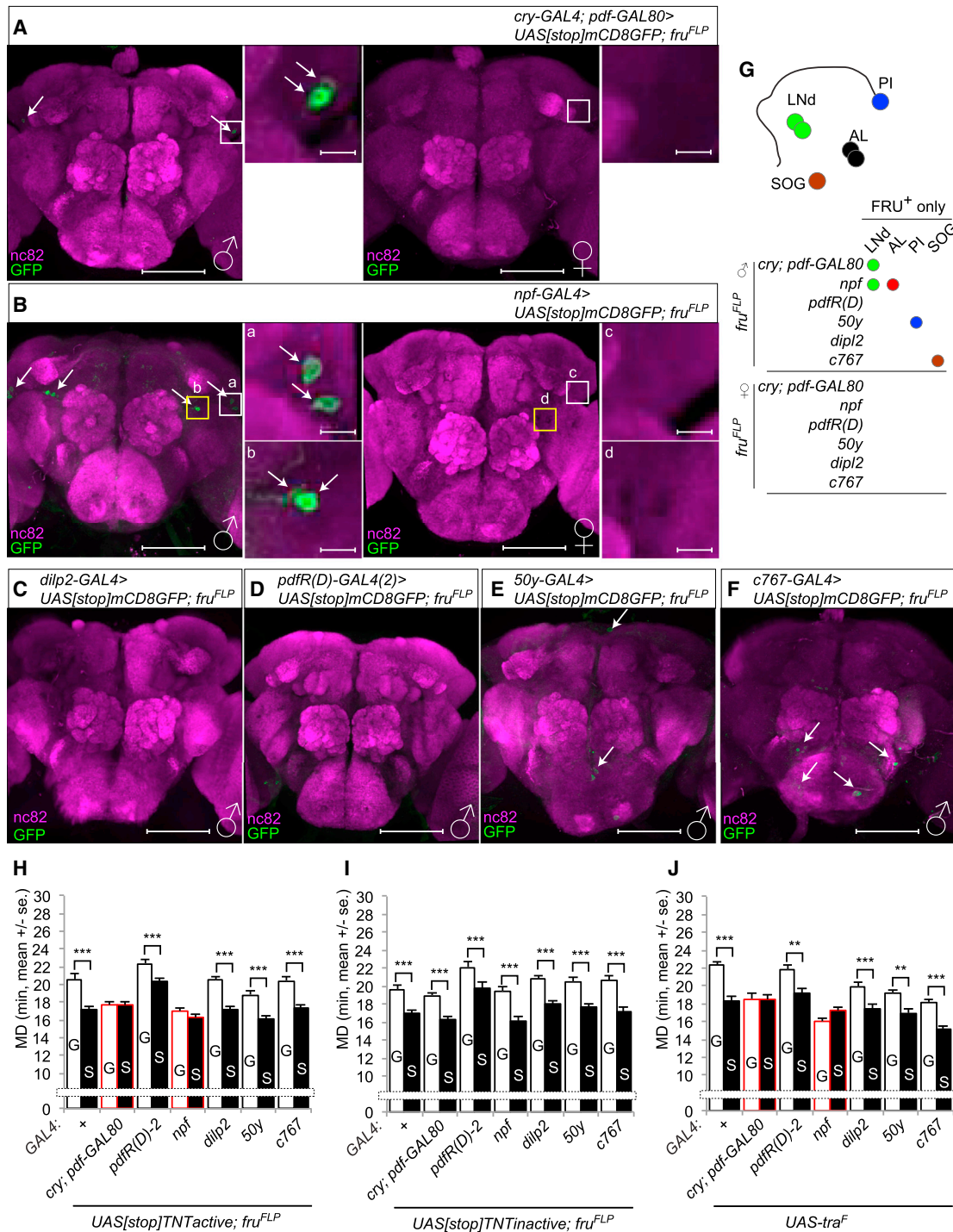
**Figure 5. Male-Specific FRU-Positive Subsets of LNd Neurons Are Required to Generate LMD**

(A–F) Flies expressing each of the *GAL4* drivers together with *UAS[stop]mCD8GFP; fru^{FLP}* were immunostained with anti-GFP (green) and nc82 (magenta) antibodies. White arrows indicate *fruitless*-positive neurons. Scale bars represent 100 μm in the left panels and 10 μm in the magnified right panels. See Figures S6F and S6G for dendrites and synaptic terminals labeled both by *npf-GAL4* and *fru^{FLP}*.

(G) Schematic diagram of sexually dimorphic cells. Subsets of neurons labeled by *GAL4* drivers (in italic) in combination with *fru^{FLP}* are color coded.

(H and I) Mating duration assays for *GAL4* drivers for inactivation of synaptic transmission via *UAS[stop]TNTactive; fru^{FLP}* (H) or control experiments with *UAS[stop]TNTinactive; fru^{FLP}* (I). Names of the *GAL4* drivers are indicated below the bars, and those that affect LMD are marked with red outline for (H)–(J).

(J) Mating duration assays for *GAL4* drivers for feminization of neurons via *UAS-tra^F*. See Figures S5A–S5G for expression pattern characterizations. Mean ± SEM is shown.

*UAS-tra^F* in other neuronal subsets (Figure 5J) or in PDF-expressing neurons or EB neurons via the *pdf-GAL4* or *c547-GAL4* driver (Figure S3D). These data suggest that LMD requires the masculine functions of a subset of neurons labeled by *cry-GAL4; pdf-GAL80* or *npf-GAL4* drivers.

Next, we asked whether *npf-GAL4*-labeled *fru*-positive LNd neurons are *cry*-positive. First, we expressed *UAS-RedStinger, UAS[stop]mCD8GFP* in combination with *fru^FLP*, so that the nuclear *RedStinger* labels all cells expressing a particular *GAL4* driver, but the *mCD8GFP* labels only those *GAL4*-expressing cells that are *fru*-positive. Among the ~12 cells labeled by *npf-GAL4* in each hemisphere, only two LNd neurons and two cells near the antenna lobe were *fru*-positive (Figure 6A). Combining *npf-GAL4* with *cry-GAL80* reduced the number of cells expressing *RedStinger* and eliminated *fru*-positive cells in the LNd region (Figure 6B). To further validate that some of the LNd neurons are *cry*-positive and *npf*-positive, we expressed *UAS-CD4-tdTomato* via the *cry-GAL4; pdf-GAL80* driver and then used anti-NPF antibody to identify two NPF-expressing cells among the four cells that were labeled by *cry-GAL4; pdf-GAL80* per hemisphere (Figure 6C). Only one *npf*-positive cell in the LNd region was *cry*-negative (Figure 6D). Because this cell was not labeled in the *fru^FLP* experiments, we conclude that only two cells are both *npf*-positive and *cry*-positive, and they are the *fru*-positive sexually dimorphic neurons in the LNd cluster (Figure 6G). We could not detect any cells that are both *npf*-positive and *pdfR*-positive in the LNd region (Figure 6E). Because *pdfR(D)-GAL4(2)*-labeled cells in the LNd region were not *fru*-positive (Figure 5D), we conclude that the two *fru*-positive, *cry*-positive and *npf*-positive cells are distinct from the two *cry*-positive and *pdfR*-positive cells in the LNd region (Figure 6G). In summary, we observe at least three types of cells in the LNd region: one cell positive for *npf* but negative for *cry*, *fru*, and *pdfR* (Figures 6B and 6D), two cells positive for *pdfR* and *cry* but negative for *npf* and *fru* (Figures 5D and 6E), and two cells positive for *npf*, *cry*, and *fru* but negative for *pdfR* (see Figures 5A, 6B–6E, and 6G for schematic diagram).

Next, we tested for the possible involvement of these three types of cells in LMD. LMD was abolished by *UAS[stop]TNT_active* expression driven by *npf-GAL4* (Figure 5H), but not by the more restricted expression imposed by the addition of *cry-GAL80* (Figure 6F). Likewise, LMD was not affected by the expression of *UAS-tra^F* via *npf-GAL4; cry-GAL80* (Figure 6F). We also confirmed that NPF expression in *cry*- and *fru*-positive neurons is important for LMD by *npf-siRNA* (Figure S3A). These studies reveal that LMD neither requires the cell in the LNd region that is positive for *npf* but negative for *cry*, *fru*, and *pdfR* nor does it require the two cells located near the antennal lobe of each hemisphere that are positive for *npf and fru* but negative for *cry* and *pdfR* (see Figures 6G and S7C for schematic diagrams). Thus, LMD requires two NPF-expressing neurons in the LNd region that are sexually dimorphic and positive for CRY but negative for PDFR (Figure 6G).

## Rival Exposure Affects the Activities of Neurons Involved in Neuropeptide Modulation of LMD

To find out whether neuronal activities are altered in neurons involved in association with LMD, we used the CaLexA (cal-cium-dependent nuclear import of LexA) system (Masuyama et al., 2012), based on the activity-dependent nuclear import of the nuclear factor of activated T cells (NFAT), a transcription factor. Because LMD requires chronic exposure to rivals for at least 6–12 hr (Kim et al., 2012), the repeated sensory inputs could conceivably result in the accumulation of the engineered transcription factor in the nuclei of active neurons in vivo.

We first examined NPF-expressing neurons because they have been implicated in LMD. Indeed, neuronal activities of some *npf-GAL4*-labeled neurons were altered by the exposure to rivals. Singly reared male flies harboring *npf-GAL4* and *LexAop-CD2-GFP; UAS-mLexA-VP16-NFAT, LexAop-CD8-GFP-2A-CD8-GFP* showed robust fluorescence in the D2 dorso-medial neurons after 5 days of social isolation. In contrast, no such signals could be detected in group-reared males. Instead, we observed fluorescent signals in a subset of LNd and l-LNv neurons in male flies exposed to rivals for 5 days (Figures 7A and 7B). Notably, group rearing increased the fluorescent signals of LNd neurons normalized by those of D2 neurons (LNd/D2 fluo-rescence) in males (Figures 7A and 7B), but not in females (Figures S6A and S6B). Moreover, group rearing did not increase the LNd/D2 fluorescence in *pdfR^hans5304* mutant males (Figure 7B), indicating that PDF signaling is crucial for this experience-dependent modulation of the activity of NPF-expressing neurons. We also failed to detect the experience-dependent increase of LNd/D2 fluorescence when CaLexA was expressed via the *cry-GAL80; npf-GAL4* driver (Figures S7D and S7E), indicating that rival exposure enhanced the activity of LNd neurons that are positive for both CRY and NPF.

Because PDF-expressing neurons are also critical for generating LMD (Kim et al., 2012), we next used the *pdf-GAL4* driver to assess their neuronal activity. The fluorescence intensity of s-LNv normalized by that of l-LNv neurons in male flies harboring *pdf-GAL4* and *LexAop-CD2-GFP; UAS-mLexA-VP16-NFAT, LexAop-CD8-GFP-2A-CD8-GFP* was decreased in group-reared males as compared to singly reared males (Figures 7C and 7D), whereas flies with *npfR1* knocked down in these neurons showed no such activity dependence on rearing conditions (Figure 7D), indicating that NPF signaling is essential for the experience-dependent modulation of the activity of PDF-ex-pressing neurons. Female flies that were group-reared or singly reared also showed no difference in neuronal activity (Figures S6C and S6D). We could not detect any fluorescence in male (Figure S6H) and female flies (Figure S6E) with the CaLexA system combined with *cry-GAL4; pdf-GAL80* or *pdfR(D)-GAL4(2)* (data not shown), most likely because of the weak *GAL4* expression. In summary, we found that exposure to rival males caused an increase of activity of the LNd neurons expressing both NPF and CRY that are required for LMD. Rival exposure also decreased the activity of s-LNv neurons expressing PDF and NPFR, when normalized by the activity of nearby l-LNv neurons.

## PDF and NPF Signaling for LMD Is Unlikely to Involve Modulation of the Expression of These Neuropeptides

Given that both PDF and NPF neuropeptides are involved in LMD, exploring the possibility of potential crosstalk at the level of PDF expression in s-LNv neurons or NPF expression in LNd neurons is of interest. The NPF expression levels of LNd neurons
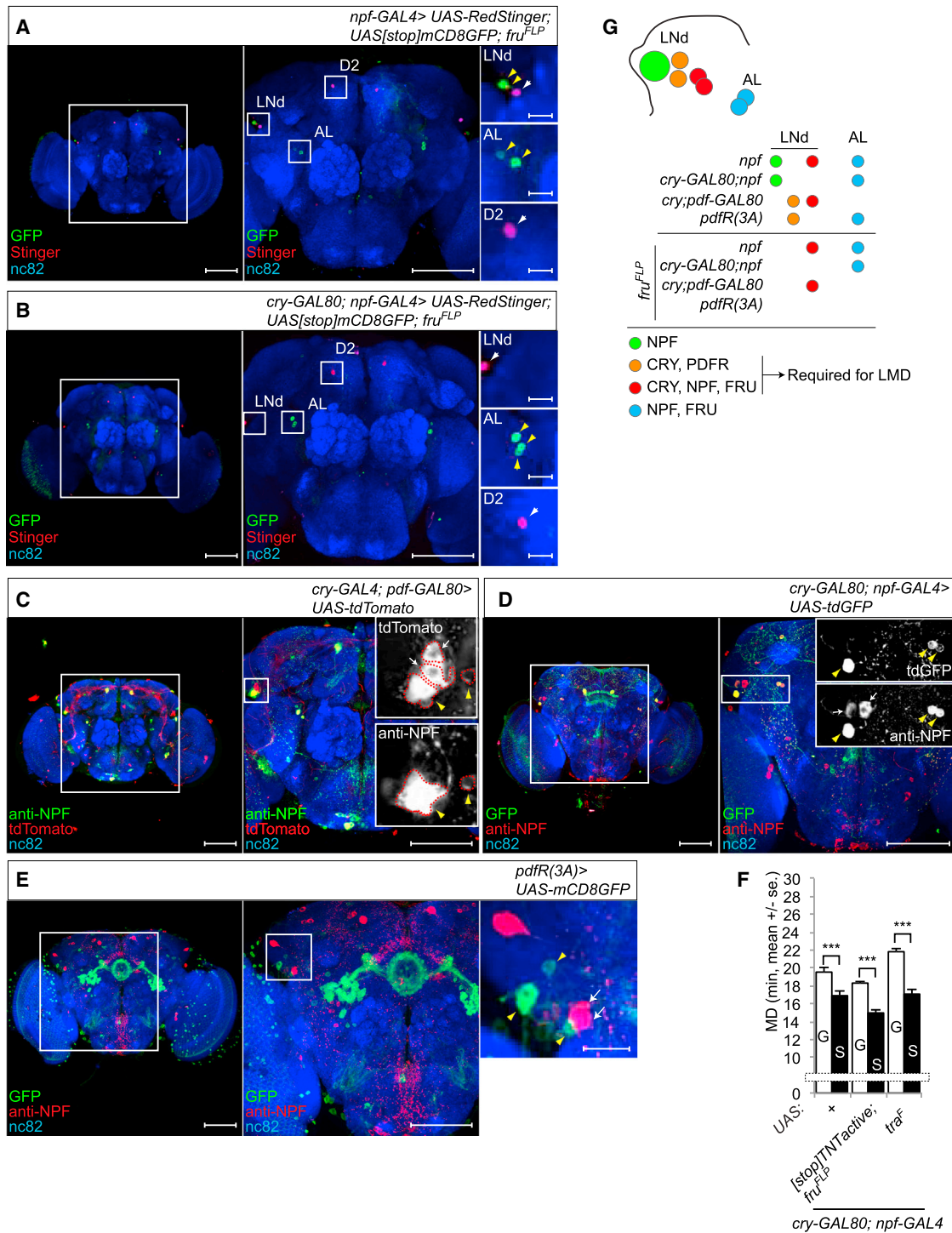
**Figure 6. NPF- and FRU-Positive Neurons that Are Required for LMD Are CRY Positive but PDFR Negative**

(A and B) FRU-positive neurons labeled by *npf-GAL4* (A) or *cry-GAL80; npf-GAL4* driver (B). Flies expressing each *GAL4* drivers together with *UAS-RedStinger; UAS[stop]mCD8GFP; fru^FLP* were immunostained with anti-GFP (green), anti-DsRed (red), and nc82 (blue) antibodies. White arrowheads indicate *GAL4*-labeled LNd neurons, and yellow arrowheads indicate additional FRU-positive neurons labeled by *GAL4* driver. Scale bars represent 100 μm in the left two panels and 10 μm in the magnified right panels.

(C) Flies expressing *cry-GAL4; pdf-GAL80* driver and *UAS-CD4-tdTomato* were immunostained with anti-NPF (green), anti-DsRed (red), and nc82 (blue) antibodies. White arrows indicate CRY-positive, NPF-negative neurons labeled by *cry-GAL4; pdf-GAL80* driver among the LNd neurons, and yellow arrowheads

*(legend continued on next page)*

normalized by those in D2 neurons were mildly reduced in *pdf* mutants compared to wild-type animals (Figures 7E and 7F). There was no change of NPF expression levels in *npfR1* mutants (Figure 7F). The PDF expression levels of s-LNv neurons normalized by those in l-LNv neurons in *npfR1* mutants were comparable to those in wild-type controls (Figure 7G). Moreover, we could not observe any differences in the expression levels of NPF or PDF between group-reared and singly reared animals (data not shown). These observations taken together with the CaLexA data support the notion that each neuropeptide modulates the activity of neurons, including those expressing the other neuropeptide, without drastically altering the expression of the other neuropeptide.

## DISCUSSION

In this study we provide evidence for the crucial involvement of two neuropeptides, PDF and NPF, in the modulation of reproductive behavior by the male's prior experience with other males. By identifying neurons required for this neuropeptide modulation, we delineate the central neuronal circuitry and find that the crucial neurons expressing a neuropeptide are not in synaptic contact with the crucial neurons expressing its receptor, providing further evidence for the long-range influence of neuropeptides. Remarkably, sharing housing with male rivals alters the activity of a subset of clock neurons, including those neurons expressing PDF and NPF that are crucial for this behavioral modulation. We also found that these altered neuronal activities of PDF- and NPF-expressing neurons in group-reared males are dependent on the signaling by NPF and PDF, respectively.

### Neuropeptides and Their Receptors in Clock Neurons Are Crucial for Rival-Induced Prolongation of Mating Duration

LMD requires PDF expression in four s-LNv neurons (Figure 1), and it also requires the expression of the NPF receptor, NPFR1, in those four s-LNv neurons (Figure 4). These four s-LNv neurons thus appear to act in the LMD generation as a relay station to receive NPF neuropeptide signaling and to transmit PDF neuropeptide signaling to neurons expressing the PDF receptor PDFR.

Unlike PDF-expressing neurons with well-known functions for circadian rhythm behavior, much less is known about neurons expressing PDFR (Im et al., 2011; Im and Taghert, 2010; Lear et al., 2005; Mertens et al., 2005; Parisky et al., 2008). To search for the PDFR-expressing cells involved in LMD, we began by identifying a small number of CRY-positive, but PDF-negative, neurons required to generate LMD (Figures 2 and S2). We then used various *pdfR-GAL4* lines to identify LNd neurons and PI neurons as candidate PDFR-expressing neurons (Figure 2). After we ruled out the involvement of PI neurons, we demonstrated that expressing PDFR in LNd neurons of *pdfR* mutants was sufficient to rescue the LMD deficits (Figure 3). Among this small group of CRY-positive, but PDF-negative, LNd neurons, two cells that express PDFR, but not NPF (Figure 5), and another distinct group of two sexually dimorphic cells that express NPF, but not PDFR (Figure 6), in each hemisphere are required for LMD. Moreover, the neuronal activities of these male-specific LNd neurons that express NPF were increased by the exposure to rivals, whereas the neuronal activity of PDF-expressing s-LNv neurons appeared to be decreased by rival exposure (Figure 7). These four s-LNv neurons also express NPFR1, which is coupled to Gi to mediate inhibition of adenylyl cylcase (Garczynski et al., 2002). Given that the rival exposure-induced alteration of s-LNv neuronal activity requires NPFR1 function (Figure 7D), one plausible scenario is that rival exposure increases the activity of NPF-expressing LNd neurons, which release NPF to activate NFPR1 on s-LNv neurons so as to reduce the activity of these PDF-expressing s-LNv neurons.

### LMD Requires PDFR Expression in Neurons that Are Not in Synaptic Contact with Crucial Neurons with PDF Expression

PDF appears to be released in a paracrine fashion to activate the G-protein-coupled receptor PDFR. PDFR is not found in the four s-LNv neurons that express PDF (Hyun et al., 2005; Lear et al., 2005; Mertens et al., 2005). One LNd neuron is known to be PDFR-positive (Hyun et al., 2005), though its PDFR signaling has not been characterized. We found that the two PDFR-expressing LNd neurons per hemisphere are crucial for LMD (Figures 2 and 3), and they do not form direct synaptic contact with the s-LNv dorsal projections (Figures 3J and S3F), consistent with the previous report that presynaptic terminals of PDF-expressing neurons have no direct contact with LNd neurons (Helfrich-Förster et al., 2007). Expression of the secreted form of PDF via an s-LNv-specific *GAL4* driver in *pdf^{01}* mutant could rescue the disrupted LMD (Figure 1E); however, expression of a membrane-tethered form of PDF could not (Figure S3H). In

indicate CRY- and NPF-positive neurons labeled by the same driver. LNd in the boxed region is magnified to clearly show two CRY- and NPF-positive neurons (yellow arrowheads) and CRY-negative and NPF-positive neurons (white arrows) with red dotted outlines. Scale bars represent 100 μm.

(D) Flies expressing *cry-GAL80; npf-GAL4* driver and *UAS-CD4-tdGFP* were immunostained with anti-GFP (green), anti-NPF (red), and nc82 (blue) antibodies. White arrows indicate CRY- and NPF-positive neurons labeled by *cry-GAL80; npf-GAL4* driver among the LNd neurons, and yellow arrowhead indicates CRY-negative and NPF-positive neurons labeled by the same driver, in the enlarged images corresponding to the boxed region in the right panel. Scale bars represent 100 μm.

(E) Flies expressing *pdfR(3A)-GAL4* and *UAS-mCD8GFP* were immunostained with anti-GFP (green), anti-NPF (red), and nc82 (blue) antibodies. White arrows indicate NPF-positive and PDFR-negative neurons labeled by *pdfR(3A)-GAL4* driver among LNd neurons, and yellow arrowheads indicate NPF-negative and PDFR-positive neurons labeled by the same driver. Scale bars represent 100 μm in the left two panels and 10 μm in the magnified right panel. See Figures S2H–S2J, S3E, S4E, S5J–S5L, S6F, S6G, and S6I for additional characterization of expression patterns.

(F) Mating duration assays for different *UAS* transgenes expressed via the *cry-GAL80; npf-GAL4 driver*. Names of the *UAS* transgenes are indicated below the bars.

(G) Schematic of LNd cells regarding their expression of NPF, CRY, PDFR, and FRU, showing that LMD requires two neurons positive for CRY and PDFR and two other neurons positive for CRY, NPF, and FRU. Subsets of neurons labeled by *GAL4* drivers (in italic) are color coded. Mean ± SEM is shown.
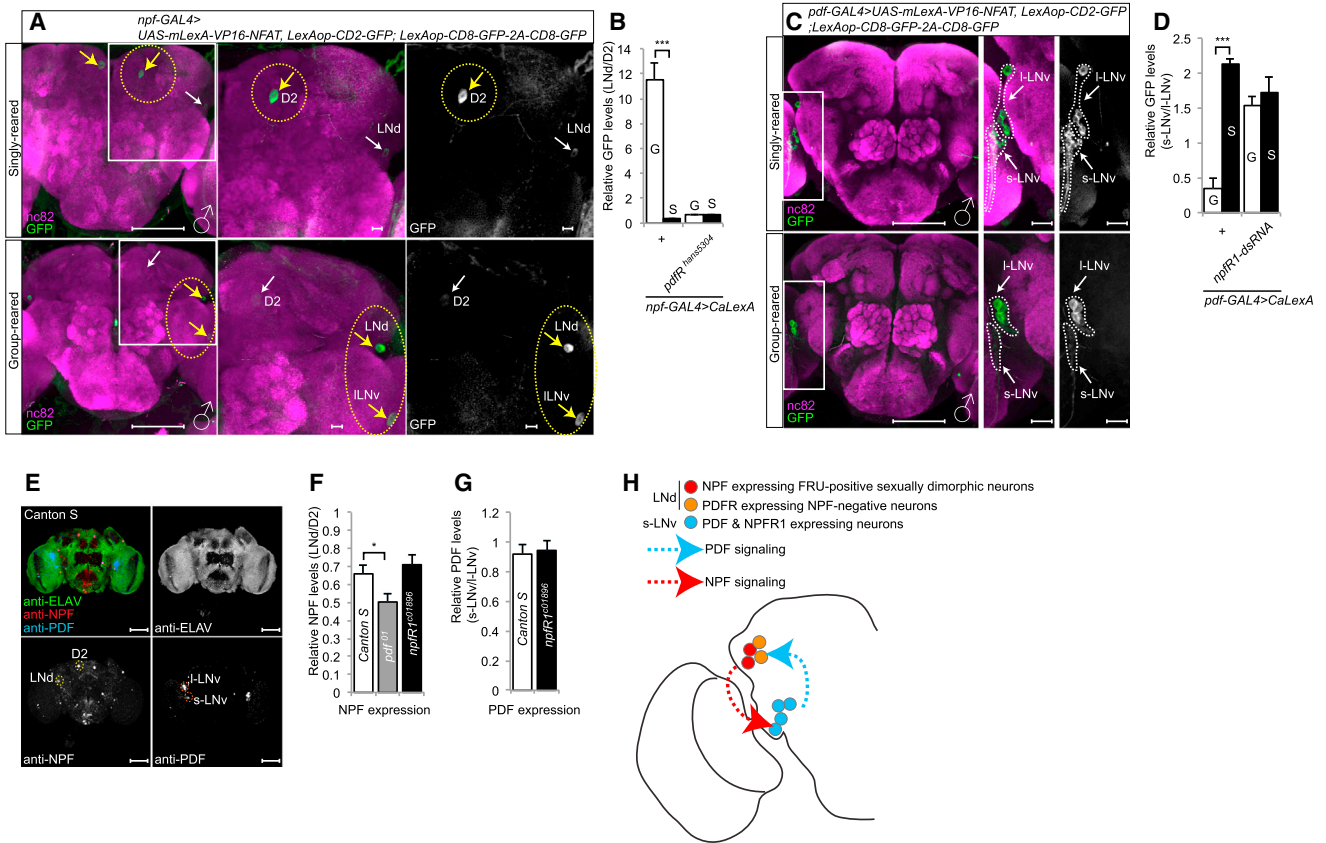
**Figure 7. Rival Experience Alters the Neural Activity of Neuropeptide-Expressing Neurons**

(A) Different levels of neural activity of LNd and l-LNv neurons as revealed by the CaLexA system in group-reared versus singly reared male flies. Flies expressing *npf-GAL4* along with *LexAop-CD2-GFP; UAS-mLexA-VP16-NFAT, LexAop-CD8-GFP-2A-CD8-GFP* were singly reared or group reared for 5 days. Brains were immunostained with anti-GFP (green) and anti-nc82 (magenta) antibodies. Yellow arrows indicate the subset of neurons showing elevated fluorescence, and white arrows indicate the subset of neurons showing reduced fluorescence in that rearing condition. Scale bars represent 100 μm in the left panel and 10 μm in the two magnified right panels.

(B) Quantification of GFP fluorescence. GFP fluorescence of LNd region is normalized by that in D2 region. Genotypes of flies were described below the bars. G, group-reared flies; S, singly reared flies. Bars represent mean of the normalized GFP fluorescence level with error bars representing the SEM. Asterisks represent significant differences revealed by a Student's t test (*p < 0.05, **p < 0.01, ***p < 0.001).

(C) Different levels of neural activity of l-LNv and s-LNv neurons as revealed by the CaLexA system in group-reared versus singly reared male flies. Flies expressing *pdf-GAL4* along with *LexAop-CD2-GFP; UAS-mLexA-VP16-NFAT, LexAop-CD8-GFP-2A-CD8-GFP* were singly reared or group reared for 5 days. Brains were immunostained with anti-GFP (green) and anti-nc82 (magenta) antibodies. White arrows indicate the l-LNvs and s-LNvs that are labeled by *pdf-GAL4* driver. Scale bars represent 100 μm in the left panel and 10 μm in the two magnified right panels.

(D) Quantification of GFP fluorescence. GFP fluorescence in the s-LNv region is normalized by that in the l-LNv region. Genotypes of flies were described below the bars. G, group-reared flies; S, singly reared flies. Bars represent mean of the normalized GFP fluorescence level with error bars representing the SEM. Asterisks represent significant differences revealed by a Student's t test (*p < 0.05, **p < 0.01, ***p < 0.001). See Figures S6A–S6E for expression in female brains and Figures S6H, S7D, and S7E for additional controls.

(E) CS male fly brain was immunostained with anti-ELAV (green), anti-NPF (red), and anti-PDF (blue) for quantification of neuropeptide expression levels. Scale bars represent 100 μm.

(F and G) Quantification of NPF (F) and PDF (G) expression levels in various fly strains. Genotypes are described inside the bars.

(H) Schematic diagram of PDF and NPF signaling among clock neurons that are required to generate LMD.

contrast, expression of a membrane-tethered form of PDF via *pdfR(D)-GAL4(2)*, with restricted expression in LNd and PI neurons, could rescue the disrupted LMD phenotype of *pdf⁰¹* mutants (Figure 3I). These results indicate that PDF secreted from s-LNv neurons can activate PDFR in LNd neurons to generate LMD. The dendrites of PDFR-positive LNd neurons labeled by *pdfR(D)-GAL4(2)* are located near the dorsal projections of PDF-expressing neurons (Figures S2F and S2G). The

dendrites of LNd neurons labeled by *50y-GAL4*, which could impair LMD when it drives the expression of *pdfR-siRNA* to reduce PDFR activity in LNd neurons, also are located near these PDF-expressing neuronal projections (Figures 3E and S2K). It has been reported that neuropeptide signaling does not require synaptic contacts. The released peptide may diffuse over tens of micrometers to reach its receptors (Jan and Jan, 1982), and the action of a peptide is limited by dilution as well as degradation/

inactivation by membrane-bound peptidases (Nässel and Winther, 2010). Thus, PDF released from s-LNv neuronal projections may signal nearby PDFR-positive LNd neurons via diffusion rather than direct synaptic contact. In summary, we identified two PDFR-positive LNd neurons per hemisphere that are responsible for generating LMD via PDF/PDFR signaling. We suggest that PDF released from s-LNv is responsible for PDFR signaling in these LNd neurons (Figures 6G and 7H).

### Rival Influences the Central Neuronal Activity of Subset of Neuropeptide-Expressing Neurons Dependent on the Signaling by the Other Neuropeptide

Our study reveals that PDF and NPF signaling is crucial for the mating duration that is controlled by the male's experience with rivals. Moreover, rival exposure greatly reduced the activity of the s-LNv neurons normalized by that of l-LNv neurons both expressing PDF but increased the activity of LNd neurons normalized by that of D2 neurons both expressing NPF (Figure 7). Interestingly, this increase in neuronal activity of NPF-positive LNd neurons in group-rearing conditions is not observed in *pdfR* mutant animals. Given that PDFR and NPF are expressed by two distinct populations of LNd neurons, the requirement of PDFR function for the rival-induced modulation of NPF-expressing neuronal activity in the LNd region raises the intriguing question of whether neuronal signaling—perhaps involving another as-yet-unidentified neuropeptide—is involved in LMD.

A recent study has identified four abdominal ganglion (AG) interneurons (INs) that contain the neuropeptide corazonin (Crz) and modulate copulation duration (Tayler et al., 2012). These neurons might play a role as a final set of effectors for the convergent effects of acute (Garbaczewska et al., 2013) and chronic (Bretman et al., 2011; Kim et al., 2012) rival competition on the copulation duration. Elucidating the neural circuitry between these AG neurons and clock neurons would be helpful in furthering our understanding of how male flies regulate mating duration in response to rivals.

Recent studies have shown that sexually dimorphic responses to pheromones in the nematode *Caenorhabditis elegans* may arise from differences in the balance of neural circuits during development (White and Jorgensen, 2012) or in the adult via neuromodulation (Jang et al., 2012). Our study adds to this emerging body of literature, illustrating the importance of sexually dimorphic neuromodulation via neuropeptide signaling in social behavior.

## EXPERIMENTAL PROCEDURES

### Mating Duration Assays

Mating duration assay was described previously (Kim et al., 2012). For group rearing, four males from the same strain were placed into a vial with food. Five CS females were collected from bottles and placed into a vial for 5 days. These females provide mating partners for mating duration assays.

Mating duration assay is performed as previously described (Yang et al., 2009). At the fifth day after eclosion, males of the appropriate strain and CS females were mildly anaesthetized by $CO_2$. After placing a single female in to the mating chamber, we inserted a transparent film then placed a single male to the other side of the film in each chamber. After allowing for 1 hr of

recovery in the mating chamber in a 25°C incubator, we removed the transparent film and recorded the mating activities. Only those males that succeeded to mate within 1 hr were included for analyses. Initiation and completion of copulation were recorded with an accuracy of 10 s, and total mating duration was calculated for each couple. All assays were performed from noon to 4 pm.

### Courtship Assay

Courtship assay was performed as previously described (Ejima and Griffith, 2007), under normal light conditions in circular courtship arenas 11 mm in diameter, from noon to 4 p.m. Courtship latency is the time between female introduction and the first obvious male courtship behavior, such as orientation coupled with wing extensions. Once courtship began, courtship index was calculated as the fraction of time a male spent in any courtship-related activity during a 10 min period or until mating occurred.

### Immunostaining and Antibodies

As described before (Lee and Luo, 1999), brains dissected from adults 5 days after eclosion were fixed in 4% formaldehyde for 30 min at room temperature, washed with 1% PBT three times (30 min each), and blocked in 5% normal donkey serum for 30 min. The brains were then incubated with primary antibodies in 1% PBT at 4°C overnight followed with fluorophore-conjugated secondary antibodies for 1 hr at room temperature. Brains were mounted with antifade mounting solution (Invitrogen, catalog #S2828) on slides for imaging. Primary antibodies used here are chicken anti-GFP (Aves Labs, 1:1,000), rabbit anti-DsRed express (Clontech, 1:250), mouse anti-Bruchpilot (nc82) (DSHB, 1:50), mouse anti-PDF (DSHB, 1:100), and rabbit anti-NPF (gift from Dr. Ping Shen, 1:2,000). Fluorophore-conjugated secondary antibodies used here are Alexa Fluor 488-conjugated goat anti-chicken (Invitrogen, 1:100), Alexa Fluor 488-conjugated donkey anti-rabbit (Invitrogen, 1:100), RRX-conjugated donkey anti-rabbit (Jackson Laboratory, 1:100), RRX-conjugated donkey anti-mouse (Jackson Laboratory, 1:100), and Dylight 649-conjugated donkey anti-mouse (Jackson Laboratory, 1:100).

### Quantitative Analysis of GFP Fluorescence

To quantify PDF and NPF levels in brain regions, we measured PDF or NPF immunofluorescence using the histogram tool of ImageJ (National Institutes of Health, http://rsb.info.nih.gov/ij). Fluorescence was quantified in a manually set region of interest (ROI) of the D2 region or LNd region (for NPF expression) and s-LNv region or l-LNv region (for PDF expression). To compensate for differences in immunofluorescence between different ROI, PDF, or NPF fluorescence was normalized to the fluorescence of anti-ELAV staining. GFP fluorescence for CaLexA was normalized to nc82 staining, and then the fluorescence of ROI was quantified using the histogram tool of ImageJ. Both hemispheres of six fly brains were analyzed (total 12) for statistical analysis. All specimens were imaged under identical conditions.

### Statistical Analysis

Statistical analysis of mating duration assay was described previously (Kim et al., 2012). More than 36 males (group- or singly reared) were used for mating duration assay. Our experience suggests that the relative mating duration differences among group- and singly reared are always consistent; however, both absolute values and the magnitude of the difference in each strain can vary. So we always include internal controls for each treatment as suggested by previous studies (Bretman et al., 2011). Therefore, statistical comparisons were made between groups that were exposed or not exposed to rivals within each experiment. As mating duration of males showed normal distribution (Kolmogorov-Smirnov tests, $p > 0.05$), we used two-sided Student's t tests. Each figure shows the mean ± SEM (***$p < 0.001$, **$p < 0.01$, *$p < 0.05$).

## SUPPLEMENTAL INFORMATION

Supplemental Information includes Supplemental Experimental Procedures and seven figures and can be found with this article online at http://dx.doi.org/10.1016/j.neuron.2013.09.034.

## REFERENCES

Beets, I., Janssen, T., Meelkop, E., Temmerman, L., Suetens, N., Rademakers, S., Jansen, G., and Schoofs, L. (2012). Vasopressin/oxytocin-related signaling regulates gustatory associative learning in C. elegans. Science *338*, 543–545.

Belote, J.M., and Baker, B.S. (1987). Sexual behavior: its genetic control during development and adulthood in Drosophila melanogaster. Proc. Natl. Acad. Sci. USA *84*, 8026–8030.

Bretman, A., Fricke, C., and Chapman, T. (2009). Plastic responses of male Drosophila melanogaster to the level of sperm competition increase male reproductive fitness. Proc. Biol. Sci. *276*, 1705–1711, Epub 2009 Feb 1725.

Bretman, A., Fricke, C., Hetherington, P., Stone, R., and Chapman, T. (2010). Exposure to rivals and plastic responses to sperm competition in Drosophila melanogaster. Behav. Ecol. *21*, 317–321.

Bretman, A., Westmancoat, J.D., Gage, M.J., and Chapman, T. (2011). Males use multiple, redundant cues to detect mating rivals. Curr. Biol. *21*, 617–622.

Burke, C.J., Huetteroth, W., Owald, D., Perisse, E., Krashes, M.J., Das, G., Gohl, D., Silies, M., Certel, S., and Waddell, S. (2012). Layered reward signalling through octopamine and dopamine in Drosophila. Nature *492*, 433–437.

Chen, J., Zhang, Y., and Shen, P. (2008). A protein kinase C activity localized to neuropeptide Y-like neurons mediates ethanol intoxication in Drosophila melanogaster. Neuroscience *156*, 42–47.

Choi, C., and Nitabach, M.N. (2010). Circadian biology: environmental regulation of a multi-oscillator network. Curr. Biol. *20*, R322–R324.

Choi, C., Fortin, J.P., McCarthy, E., Oksman, L., Kopin, A.S., and Nitabach, M.N. (2009). Cellular dissection of circadian peptide signals with genetically encoded membrane-tethered ligands. Current biology: CB *19*, 1167–1175.

Choi, S., Chatzigeorgiou, M., Taylor, K.P., Schafer, W.R., and Kaplan, J.M. (2013). Analysis of NPR-1 reveals a circuit mechanism for behavioral quiescence in C. elegans. Neuron *78*, 869–880.

Dierick, H.A., and Greenspan, R.J. (2007). Serotonin and neuropeptide F have opposite modulatory effects on fly aggression. Nat. Genet. *39*, 678–682.

Ejima, A., and Griffith, L.C. (2007). Measurement of courtship behavior in Drosophila melanogaster. Cold Spring Harb. Protoc. *2007*, http://dx.doi.org/10.1101/pdb.prot4847.

Feinberg, E.H., Vanhoven, M.K., Bendesky, A., Wang, G., Fetter, R.D., Shen, K., and Bargmann, C.I. (2008). GFP Reconstitution Across Synaptic Partners (GRASP) defines cell contacts and synapses in living nervous systems. Neuron *57*, 353–363.

Garbaczewska, M., Billeter, J.C., and Levine, J.D. (2013). Drosophila melanogaster males increase the number of sperm in their ejaculate when perceiving rival males. J. Insect Physiol. *59*, 306–310.

Garczynski, S.F., Brown, M.R., Shen, P., Murray, T.F., and Crim, J.W. (2002). Characterization of a functional neuropeptide F receptor from Drosophila melanogaster. Peptides *23*, 773–780.

Garrison, J.L., Macosko, E.Z., Bernstein, S., Pokala, N., Albrecht, D.R., and Bargmann, C.I. (2012). Oxytocin/vasopressin-related peptides have an ancient role in reproductive behavior. Science *338*, 540–543.

Han, C., Jan, L.Y., and Jan, Y.N. (2011). Enhancer-driven membrane markers for analysis of nonautonomous mechanisms reveal neuron-glia interactions in Drosophila. Proc. Natl. Acad. Sci. USA *108*, 9673–9678.

Helfrich-Förster, C., Shafer, O.T., Wülbeck, C., Grieshaber, E., Rieger, D., and Taghert, P. (2007). Development and morphology of the clock-gene-expressing lateral neurons of Drosophila melanogaster. J. Comp. Neurol. *500*, 47–70.

Hermann, C., Yoshii, T., Dusik, V., and Helfrich-Förster, C. (2012). Neuropeptide F immunoreactive clock neurons modify evening locomotor activity and free-running period in Drosophila melanogaster. J. Comp. Neurol. *520*, 970–987.

Hidalgo, A., Urban, J., and Brand, A.H. (1995). Targeted ablation of glia disrupts axon tract formation in the Drosophila CNS. Development *121*, 3703–3712.

Hyun, S., Lee, Y., Hong, S.T., Bang, S., Paik, D., Kang, J., Shin, J., Lee, J., Jeon, K., Hwang, S., et al. (2005). Drosophila GPCR Han is a receptor for the circadian clock neuropeptide PDF. Neuron *48*, 267–278.

Im, S.H., and Taghert, P.H. (2010). PDF receptor expression reveals direct interactions between circadian oscillators in Drosophila. J. Comp. Neurol. *518*, 1925–1945.

Im, S.H., Li, W., and Taghert, P.H. (2011). PDFR and CRY signaling converge in a subset of clock neurons to modulate the amplitude and phase of circadian behavior in Drosophila. PLoS ONE *6*, e18974.

Insel, T.R. (2010). The challenge of translation in social neuroscience: a review of oxytocin, vasopressin, and affiliative behavior. Neuron *65*, 768–779.

Jan, L.Y., and Jan, Y.N. (1982). Peptidergic transmission in sympathetic ganglia of the frog. J. Physiol. *327*, 219–246.

Jang, H., Kim, K., Neal, S.J., Macosko, E., Kim, D., Butcher, R.A., Zeiger, D.M., Bargmann, C.I., and Sengupta, P. (2012). Neuromodulatory state and sex specify alternative behaviors through antagonistic synaptic pathways in C. elegans. Neuron *75*, 585–592.

Kadener, S., Villella, A., Kula, E., Palm, K., Pyza, E., Botas, J., Hall, J.C., and Rosbash, M. (2006). Neurotoxic protein expression reveals connections between the circadian clock and mating behavior in Drosophila. Proc. Natl. Acad. Sci. USA *103*, 13537–13542.

Kim, W.J., Jan, L.Y., and Jan, Y.N. (2012). Contribution of visual and circadian neural circuits to memory for prolonged mating induced by rivals. Nat. Neurosci. *15*, 876–883.

Krashes, M.J., DasGupta, S., Vreede, A., White, B., Armstrong, J.D., and Waddell, S. (2009). A neural circuit mechanism integrating motivational state with memory expression in Drosophila. Cell *139*, 416–427.

Lear, B.C., Merrill, C.E., Lin, J.M., Schroeder, A., Zhang, L., and Allada, R. (2005). A G protein-coupled receptor, groom-of-PDF, is required for PDF neuron action in circadian behavior. Neuron *48*, 221–227.

Lee, T., and Luo, L. (1999). Mosaic analysis with a repressible cell marker for studies of gene function in neuronal morphogenesis. Neuron *22*, 451–461.

Lee, G., Bahn, J.H., and Park, J.H. (2006). Sex- and clock-controlled expression of the neuropeptide F gene in Drosophila. Proc. Natl. Acad. Sci. USA *103*, 12580–12585.

Lee, K.S., Kwon, O.Y., Lee, J.H., Kwon, K., Min, K.J., Jung, S.A., Kim, A.K., You, K.H., Tatar, M., and Yu, K. (2008). Drosophila short neuropeptide F signalling regulates growth by ERK-mediated insulin signalling. Nat. Cell Biol. *10*, 468–475.

Lingo, P.R., Zhao, Z., and Shen, P. (2007). Co-regulation of cold-resistant food acquisition by insulin- and neuropeptide Y-like systems in Drosophila melanogaster. Neuroscience *148*, 371–374.

Masuyama, K., Zhang, Y., Rao, Y., and Wang, J.W. (2012). Mapping neural circuits with activity-dependent nuclear import of a transcription factor. J. Neurogenet. *26*, 89–102.

Mertens, I., Vandingenen, A., Johnson, E.C., Shafer, O.T., Li, W., Trigg, J.S., De Loof, A., Schoofs, L., and Taghert, P.H. (2005). PDF receptor signaling in Drosophila contributes to both circadian and geotactic behaviors. Neuron *48*, 213–219.

Nagoshi, E., Sugino, K., Kula, E., Okazaki, E., Tachibana, T., Nelson, S., and Rosbash, M. (2010). Dissecting differential gene expression within the circadian neuronal circuit of Drosophila. Nat. Neurosci. *13*, 60–68.

Nässel, D.R. (2000). Functional roles of neuropeptides in the insect central nervous system. Naturwissenschaften *87*, 439–449.

Nässel, D.R., and Winther, A.M. (2010). Drosophila neuropeptides in regulation of physiology and behavior. Prog. Neurobiol. *92*, 42–104.

Nicolaï, L.J., Ramaekers, A., Raemaekers, T., Drozdzecki, A., Mauss, A.S., Yan, J., Landgraf, M., Annaert, W., and Hassan, B.A. (2010). Genetically encoded dendritic marker sheds light on neuronal connectivity in Drosophila. Proc. Natl. Acad. Sci. USA *107*, 20553–20558.

Nitabach, M.N., and Taghert, P.H. (2008). Organization of the Drosophila circadian control circuit. Current biology: CB *18*, R84–R93.

O'Brien, M.A., and Taghert, P.H. (1998). A peritracheal neuropeptide system in insects: release of myomodulin-like peptides at ecdysis. J. Exp. Biol. *201*, 193–209.

Parisky, K.M., Agosto, J., Pulver, S.R., Shang, Y., Kuklin, E., Hodge, J.J., Kang, K., Liu, X., Garrity, P.A., Rosbash, M., and Griffith, L.C. (2008). PDF cells are a GABA-responsive wake-promoting component of the Drosophila sleep circuit. Neuron *60*, 672–682.

Pfeiffer, B.D., Jenett, A., Hammonds, A.S., Ngo, T.T., Misra, S., Murphy, C., Scully, A., Carlson, J.W., Wan, K.H., Laverty, T.R., et al. (2008). Tools for neuroanatomy and neurogenetics in Drosophila. Proc. Natl. Acad. Sci. USA *105*, 9715–9720.

Renn, S.C., Park, J.H., Rosbash, M., Hall, J.C., and Taghert, P.H. (1999). A pdf neuropeptide gene mutation and ablation of PDF neurons each cause severe abnormalities of behavioral circadian rhythms in Drosophila. Cell *99*, 791–802.

Ryner, L.C., Goodwin, S.F., Castrillon, D.H., Anand, A., Villella, A., Baker, B.S., Hall, J.C., Taylor, B.J., and Wasserman, S.A. (1996). Control of male sexual behavior and sexual orientation in Drosophila by the fruitless gene. Cell *87*, 1079–1089.

Shen, P., and Cai, H.N. (2001). Drosophila neuropeptide F mediates integration of chemosensory stimulation and conditioning of the nervous system by food. J. Neurobiol. *47*, 16–25.

Shohat-Ophir, G., Kaun, K.R., Azanchi, R., Mohammed, H., and Heberlein, U. (2012). Sexual deprivation increases ethanol intake in Drosophila. Science *335*, 1351–1355.

Taghert, P.H., and Nitabach, M.N. (2012). Peptide neuromodulation in invertebrate model systems. Neuron *76*, 82–97.

Tayler, T.D., Pacheco, D.A., Hergarden, A.C., Murthy, M., and Anderson, D.J. (2012). A neuropeptide circuit that coordinates sperm transfer and copulation duration in Drosophila. Proc. Natl. Acad. Sci. USA *109*, 20697–20702.

Venken, K.J., Popodi, E., Holtzman, S.L., Schulze, K.L., Park, S., Carlson, J.W., Hoskins, R.A., Bellen, H.J., and Kaufman, T.C. (2010). A molecularly defined duplication set for the X chromosome of Drosophila melanogaster. Genetics *186*, 1111–1125.

Wen, T., Parrish, C.A., Xu, D., Wu, Q., and Shen, P. (2005). Drosophila neuropeptide F and its receptor, NPFR1, define a signaling pathway that acutely modulates alcohol sensitivity. Proc. Natl. Acad. Sci. USA *102*, 2141–2146.

White, J.Q., and Jorgensen, E.M. (2012). Sensation in a single neuron pair represses male behavior in hermaphrodites. Neuron *75*, 593–600.

Wu, Q., Wen, T., Lee, G., Park, J.H., Cai, H.N., and Shen, P. (2003). Developmental control of foraging and social behavior by the Drosophila neuropeptide Y-like system. Neuron *39*, 147–161.

Wu, Q., Zhao, Z., and Shen, P. (2005a). Regulation of aversion to noxious food by Drosophila neuropeptide Y- and insulin-like systems. Nat. Neurosci. *8*, 1350–1355.

Wu, Q., Zhang, Y., Xu, J., and Shen, P. (2005b). Regulation of hunger-driven behaviors by neural ribosomal S6 kinase in Drosophila. Proc. Natl. Acad. Sci. USA *102*, 13289–13294.

Yang, C.H., Rumpf, S., Xiang, Y., Gordon, M.D., Song, W., Jan, L.Y., and Jan, Y.N. (2009). Control of the postmating behavioral switch in Drosophila females by internal sensory neurons. Neuron *61*, 519–526.